NASA Technical Paper 1099

Recovery and Radiation Corrections and Time Constants of Several Sizes of Shielded and Unshielded Thermocouple Probes for Measuring Gas Temperature

George E. Glawe, Raymond Holanda,
and Lloyd N. Krause

JANUARY 1978

NASA

NASA Technical Paper 1099

Recovery and Radiation Corrections and Time Constants of Several Sizes of Shielded and Unshielded Thermocouple Probes for Measuring Gas Temperature

George E. Glawe, Raymond Holanda, and Lloyd N. Krause

Lewis Research Center
Cleveland, Ohio

National Aeronautics and Space Administration

Scientific and Technical Information Office

1978

RECOVERY AND RADIATION CORRECTIONS AND TIME CONSTANTS OF SEVERAL SIZES OF SHIELDED AND UNSHIELDED THERMOCOUPLE PROBES FOR MEASURING GAS TEMPERATURE

by George E. Glawe, Raymond Holanda, and Lloyd N. Krause

Lewis Research Center

SUMMARY

Radiation and recovery corrections and time constants were experimentally determined for several sizes of a shielded and unshielded thermocouple probe design. The probes were of swaged construction and were made of type K wire with a stainless-steel sheath and shield and magnesium oxide (MgO) insulation. The wire sizes ranged from 0.03- to 1.02-millimeter diameter for the unshielded design and from 0.16- to 0.81-millimeter diameter for the shielded design. The probes were tested through a Mach number range of 0.2 to 0.9, over a temperature range of room ambient to 1420 K, and through a total-pressure range of 0.03 to 0.22 megapascal (0.3 to 2.2 atm). Measured time constants ranged from 0.03 to 1.7 seconds. Radiation correction ranged from 11 to 138 K. Reference recovery correction factors, at Mach 0.9, ranged from 0.002 to 0.028. The unshielded design had a smaller time constant, and the recovery characteristics were less affected by flow misalinement and by operation over a large pressure range. The shielded probes afforded better physical protection to the thermocouple elements and have, for the larger sizes, substantially decreased radiation and recovery corrections. Tables and graphs are presented that compare the characteristics of various probe sizes as an aid in selecting a particular type and size.

INTRODUCTION

The work discussed in this report was performed to standardize the thermocouple probe designs used at the Lewis Research Center for the temperature range from ambient to 1400 K. One of the major cost factors in producing thermocouple probes is the expense of calibration. By standardizing a relatively few designs and sizes and extensively tabulating the various measurement correction factors for each design and size, the overall requirements for extensive calibrations should be greatly diminished.

The choice of a thermocouple probe for a particular application involves a compromise between many features involving mechanical and operational characteristics (refs. 1 to 5). One of the main considerations from the mechanical point of view is the size of a particular probe since the size is directly related to such factors as cost, strength, installation considerations, fatigue life, and aerodynamic loading and blockage. Size also enters into the operational characteristics of the probe through such factors as the time constant, recovery factor, and conductive and radiative heat exchange.

The present effort is an extension of earlier work (ref. 4) in that it draws on the basic design of two of the earlier probes and uses the same apparatus, procedure, and analysis to examine a range of sizes of these two designs. Ten sizes of unshielded and five sizes of shielded wedge-type probes were tested. The wire sizes ranged from 0.03- to 1.02-millimeter diameter for the unshielded design and from 0.16- to 0.81-millimeter diameter for the shielded design. Recovery tests were performed at room temperature over a Mach number range of 0.2 to 0.9 and over a total-pressure range of 0.03 to 0.22 megapascal (0.3 to 2.2 atm). Yaw angle effects were tested to $\pm 30^{\circ}$, and pitch angle effects were tested to $\pm 15^{\circ}$. Time-constant tests were performed over a Mach number range of 0.3 to 0.6. Radiation error tests were performed over a temperature range of 810 to 1420 K, a Mach number range of 0.2 to 0.8, and a pressure range of 0.07 to 0.13 megapascal (0.7 to 1.3 atm).

PROBE DESIGN CONSIDERATIONS

Detailed drawings of the wedge-type unshielded and shielded thermocouple probes are shown in figure 1 with related dimensions in table I. Ten different sizes of the unshielded-probe design were made using swaged thermocouple construction, with nominal wire sizes ranging from 0.03- to 1.02-millimeter diameter. Five different sizes of the shielded-probe design were made using swaged thermocouple construction, with nominal wire sizes ranging from 0.16- to 0.81-millimeter diameter. The 10 sizes of unshielded probes were identified by numbering them from 1 to 10. The five sizes of shielded probes were made by welding cylindrical shields onto unshielded assemblies whose corresponding numbers are 4, 6, 7, 8, and 9 (table I). Figure 2 shows probes 1 and 10 (unshielded design) and probes 4 and 9 (shielded design) to illustrate the size range for each type. Two probes of each size and type were constructed for the tests.

One of the main ground rules for the standardization program was to use commercially available swaged thermocouple assemblies with stainless-steel sheaths, MgO insulation, and type K (e.g., Chromel-Alumel) wire. It was also desired to use off-the-shelf stainless-steel tubing sizes for fabricating the shields.

The thermocouple junctions were formed by gas tungsten-arc welding equipment;

for the two thinnest wires (probes 1 and 2) the high-frequency starter arc alone provided sufficient power to weld the junctions.

General design dimensions were based on performance characteristics of various shielded- and unshielded-probe designs previously developed and tested at the Lewis Research Center and include both analytical and experimental source information. The following discussion of the choice of design parameters can only be generalized, since many compromises were involved and all applications could not be anticipated and covered by a standard design. This discussion is included to aid the reader in scaling the designs to other sizes and to explain what considerations went into the dimensional relationships.

Exposed Thermocouple Wire Length

A primary consideration in the length of wire loop exposed is the degree of conductive heat loss from the junction, through the wire, to the swaged support assembly. Reference 2 shows that a conduction loss factor is inversely related to the square of the ratio of wire length to wire diameter. The length-to-diameter ratio would be restricted by the effects of vibration, temperature, and aerodynamic loading (especially under non-alined-flow conditions), which could cause bending and structural failure. In addition, a large junction weld bead would augment these effects, since it would put a concentrated load at the extremity of the cantilevered wires. The probes discussed in this report had an exposed wire length (each leg) of 15 times the wire diameter. This is dimension Z of table I. Experience has shown this length to be a practical compromise for most applications. This length may not be adequate for some applications where low pressure (<0.02 MPa (<0.2 atm)) along with low Mach number (<0.2) exist and where considerable conductive heat transfer (large ΔT between junction and support) is present. Reference 2 can be used to estimate this error and to aid in redesigning for a longer wire when necessary.

Shield Design Parameters

The tip of the thermocouple junction is positioned 1 shield outside diameter distant from the shield inlet. This position was not analytically or experimentally optimized but represents a judgment based on consideration of entrance flow effects, radiation shielding geometry, and convective heat transfer between thermocouple and shield. In regard to flow effects, if the junction were placed too near the plane of the entrance, it would probably be disturbed by nonalined flow. In respect to radiation shielding, the shield would become more effective if the junction wire moved back from

the entrance because the shield subtends a larger solid angle at the wire. If the distance from the entrance to the junction were made too long, it is possible for the incoming gas to lose heat to the shield and be at a lower temperature when it reaches the junction.

The probe support was bent at a right angle in order to place the exposed thermocouple wire parallel to the gas flow. For the shielded probes, this forward-facing portion of the probe must have a straight section whose length is at least 1 shield outside diameter. The shield overlaps this length. Total shield length (V in fig. 1) is therefore equal to exposed wire length Z plus 2 shield outside diameters.

The shield bleed holes were located just forward of the plane where the two wires enter the insulation of the swaged support assembly (called the "base" of the thermocouple). This location allows the gas to pass over as much of the exposed thermocouple wire as possible. However, experience has shown that it is questionable practice to design a shielded probe of this type with the back edge of the bleed hole touching the plane of the wire-base interface. Partial bleed-hole blockage will occur if the shield is pushed too far onto the support during assembly. To help circumvent this, the centerline of the bleed hole was located a distance X (fig. 1) equal to 1 bleed-hole diameter from the base interface. This allows an assembly tolerance of 1/2 bleed-hole diameter. A second consideration is to prevent or delay bleed-hole blockage by possible accretion of stream particulates on the insulator interface.

Shield bleed-hole area involves a compromise between recovery correction on one hand and radiation correction and time response on the other. For the shielded probes in this report, the total bleed-hole area was nominally 50 percent of the shield inlet area. However, experience has shown that bleed holes may become plugged by stream particulates when bleed-hole diameter is less than 0.5 millimeter. To keep bleed-hole size above this value and still maintain the standard 50-percent bleed ratio, the two smaller shielded probes had only two bleed holes rather than the symmetrical four-bleed-hole arrangement of the larger probes.

Table II summarizes the design constraints placed on the dimensions shown in figure 1 and table I.

Although these probes were tested as individual units, the design is such that it lends itself to "stacking" to form a multisensing probe assembly (fig. 3). The probes may be clustered as shown and merely welded together or, in addition, an airfoil-shaped housing (dashed line) or a metal-fill area (crosshatching) can be used. This grouping has two advantages over a single element; it increases the section modulus of the support region, thereby adding strength, and it also decreases the support's aerodynamic drag coefficient over that of a single element. Both of these factors decrease the amount that the probe will bend under a given condition of aerodynamic loading.

The width (dimension B) of the support structure on the rake assembly is only slightly wider than the nominal outside diameter of the swaged assembly. The local Mach number in the region of the sensor is a function of stream Mach number and support shape and frontal area. In one case, a rake assembly using a probe 4 shielded design was fabricated with an airfoil support structure twice the nominal width. A calibration with this wider support (unpublished data) showed a 20 percent decrease in the recovery correction factor as compared with a standard probe.

Two additional modified designs were used to investigate how variations in the shield design affected the radiation correction. In one of the modified designs, the shield size was kept the same as that of a standard probe, but the bleed area was increased from the standard 50 percent to 100 percent of the inlet area. In the second modified design the shield size was increased so that the inlet area was eight times that of the standard probe (but with the bleed-area-to-inlet-area ratio remaining at 50 percent).

APPARATUS AND PROCEDURE

Recovery Test Apparatus

Recovery correction factors were determined in the apparatus shown schematically in figure 4. The flow process in the nozzle and testing regions was isentropic within the accuracy of the pressure and temperature measurements. Tests were made at room total temperatures of 295 to 310 K. Probable measurement error in total temperature was 0.6 K. The recovery correction was measured with a differential circuit formed between a thermocouple in the plenum and the test probe in the jet, with an inaccuracy of ±0.06 K. Errors in pressure measurement were negligible.

In order to prevent excessive bending of the smaller probes as a result of aerodynamic loading, depth of support stem immersion in the airstream was decreased with probe size.

Time-Constant Test Apparatus

Time-constant determinations were made in the apparatus shown in figure 5. The probe was preheated to a constant temperature with a hot-air blower while it was protected from the airstream by a shield. The shield was then pneumatically retracted to halt the flow of hot air. The result is a step change in applied temperature, with the probe output responding in the familiar exponential cooling curve.

Radiation Test Apparatus

Radiation corrections were determined in the high-temperature tunnel shown in figure 6. This facility uses natural gas as a fuel and is capable of producing test section conditions of Mach 0.2 to 0.9 at temperatures from 810 to 1860 K and at total pressures from 0.05 to 0.2 megapascal (0.5 to 2 atm). The radiation testing was done by comparing the test probe with an accurate reference probe. This was accomplished at any given stream condition by moving each probe in turn to the same location in the gas stream. The reference probe used to determine total temperature was a double-shielded aspirated probe (ref. 6). The radiation correction for the test probe was then taken as the difference between the total temperature (as determined by the reference probe) and the indicated test probe temperature adjusted for recovery correction.

In the radiation tests a fixed probe length had to be used in order to position the element in the center of the output of the high-temperature jet. It was necessary therefore to back up the smaller probes (4 to 6) with a thin sheet-metal bracket. Probes 1 to 3 were not tested because their radiation corrections were so small. Also because of structural and wire strength considerations, probe 4 was run below 1310 K and below Mach 0.55, and test conditions were systematically increased to 1420 K and Mach 0.8 for probe 10.

TESTS AND RESULTS

Recovery, time-constant, and radiation tests were run on the probes. The probes were made from available swaged assembly stock. Some of the wire sizes (for a specified sheath outside diameter) varied more than 1 wire gage size from the nominal wire sizes listed in table I. Experimental results in the accompanying figures were therefore plotted according to the actual wire size. To relate back to design nominal sizes, selected values for the nominal wire sizes were then obtained from curves faired through the experimental data. These data are tabulated and identified as "smoothed values."

Recovery Correction Factor

In using thermocouple probes, it is convenient to correct for an aerodynamic recovery error by using a recovery correction factor Δ.

$$\Delta = \frac{T_t - T_i}{T_t} \tag{1}$$

where T_t is the total temperature and T_i is the indicated thermocouple temperature. All temperatures are absolute. In an application in which the thermocouple junction has responded to the aerodynamic flow and where conductive and radiative heat exchange are not present, the quantity T_i is equal to the adiabatic junction temperature, and T_t can be calculated from the indicated junction temperature and the value of Δ.

$$T_t = \frac{T_i}{1 - \Delta} \tag{2a}$$

and since $\Delta \ll 1$ for a well-designed probe

$$T_t \approx T_i(1 + \Delta) \tag{2b}$$

The recovery correction factor of a thermocouple probe, in alined flow, varies primarily with stream Mach number, with a secondary effect of stream pressure. The recovery correction factor for alined flow, at 0.1-megapascal (1-atm) stream total pressure, is termed the reference recovery correction factor Δ_0.

Reference recovery correction factor for unshielded probes. - The variation of Δ_0 with Mach number for the 10 sizes of unshielded probes is presented in figure 7 as a band encompassing all the data points. A mean-value curve is drawn through this envelope. The limit of scatter around the mean value is about ±10 percent of Δ_0 at Mach 0.2 to 0.5 and increases to about ±25 percent of Δ_0 at Mach 0.9. The maximum difference between any two probes of a given size, because of variation in construction, was about ±10 percent. To Mach 0.5, the use of the mean value of Δ_0 from the curve of figure 7 is justifiable for all 10 probe sizes since this implies a limit of uncertainty in temperature measurement less than 0.08 percent. At Mach 0.9, the limit of uncertainty becomes 0.6 percent.

Reference recovery correction factors at selected Mach numbers for each unshielded probe are given in table III. The numbers represent the average of the two probes tested in each size. There is no clearly significant effect of probe size. The effect of junction weld bead size for the smaller probes is elaborated on in the discussion section.

Reference recovery correction factor for shielded probes. - The variation of Δ_0 with Mach number for the five sizes of shielded probes is presented in figure 8 as a band encompassing all the data points. A mean curve is drawn through the envelope. The limit of scatter around the mean value is about ±40 percent of Δ_0; but since the absolute value of Δ_0 is so small (0.005 maximum), the 40-percent variation results in less than 0.2 percent uncertainty in the absolute value of total temperature.

Reference recovery correction factors at selected Mach numbers for each shielded

probe are given in table IV. The values represent the average of the two probes tested in each size. The smallest shielded probe (4) had the highest Δ_0, the largest shielded probe (9) had the smallest Δ_0, and the remaining shielded probes (6, 7, and 8) exhibited identical values close to the mean-value line.

Pressure effect on recovery for unshielded probes. - The variation of recovery correction factor with pressure for the unshielded probes is shown in figure 9. One probe of each size was tested at Mach 0.3, 0.6, and 0.9. The data are presented as a band encompassing all the points for probes 2 to 10 and follow a pattern similar to previous results (ref. 4). However, probe 1, shown as a dashed line, does not follow this trend. This matter is treated in the discussion section. For probes larger than probe 1, a recovery factor chosen from the mean-value curve in figure 9 would not be in error by more than 15 percent of Δ.

Pressure effect on recovery for shielded probes. - The variation of recovery correction factor with pressure for the shielded probes is shown in figure 10. Again, one probe of each size was tested at Mach 0.3, 0.6, and 0.9. The data are presented as a band encompassing all the points. A recovery factor chosen from the mean-value curve in figure 10 would not be in error by more than 20 percent of Δ. No systematic effects of probe size were seen.

Temperature effect on recovery. - No experimental work was done to determine the effect of temperature on recovery. The temperature effect for the probes of this report is treated in the discussion section.

Yaw effect on recovery for unshielded probes. - Figure 11 shows the effect of yaw angle on recovery correction factor for the 10 sizes of the unshielded wedge thermocouple design. The data are presented as a band encompassing all the points. Within a yaw angle of $\pm 30^{\circ}$, the recovery correction factor never varied by more than 20 percent from its zero angle value. This yaw angle range should cover most of the applications of these probes.

No systematic variation in yaw angle effect on recovery with probe size was observed; but there was considerable variation in yaw angle effect between two probes of the same size. Therefore, it will be necessary to calibrate each probe individually in order to determine its characteristics, if the uncertainties shown in figure 11 are too great for a user's needs. The data of figure 11 include recovery correction factors determined at Mach 0.3, 0.6, and 0.9 for each probe tested, and no systematic variation in $\Delta/\Delta_{\beta=0}$ with Mach number was observed.

Yaw effect on recovery for shielded probes. - Figure 12 shows the effect of yaw angle on recovery correction factor for the five sizes of shielded probes. The data are presented as a band encompassing all the points. A mean curve is drawn through the envelope. For a yaw angle of about $\pm 10^{\circ}$, the effect is not serious, but beyond these limits the shield begins to cut the flow to the thermocouple junction and the effect

becomes very significant. The recovery correction factor is nearly doubled at $\pm 30^{\circ}$. It is therefore advisable to aline these probes accurately in their installation. No systematic effect of probe size on the yaw angle effect was noted.

Pitch effect on recovery of unshielded and shielded probes. - Pitch data were obtained for various selected sizes of the probes to $\pm 15^{\circ}$ and, in general, fell within the shaded envelope of yaw data presented in figure 11 for the unshielded probes and in figure 12 for the shielded probes. Since pitch angles exceeding 15° are unlikely in most practical applications, no separate tables or graphs are presented for the effect of pitch.

Time Constant

Reference 4 gives a relation to approximate the time constant τ for a simple thermocouple probe configuration, which can be expressed as

$$\tau \approx \frac{\tau_0}{\sqrt{Mp/p_0}} \left(\frac{T_i}{T_0} \right)^{-0.18} \tag{3}$$

where

τ_0 reference time constant for particular probe

M stream Mach number

p stream static pressure, MPa (atm)

p_0 reference static pressure, 0.1 MPa (1 atm)

T_i probe indicated temperature, K

T_0 reference temperature, 555 K

Time constants τ were experimentally measured for two of each size of the shielded and unshielded probes by using the apparatus shown in figure 5. The τ_0 value for each probe was then calculated by using equation (3). After the τ_0 value is established for each particular probe, it may be used in equation (3) to approximate the time constant for other conditions where Mach number, pressure, and indicated temperatures are known.

Time constant for unshielded probes. - The experimentally determined reference time constants τ_0 for the 10 unshielded probes are presented in figure 13 as a function of actual wire diameter. Each point represents the average value for the two probes tested. A curve is fit through the data, and the value for each particular probe taken

from the curve fit is presented in table V as a function of nominal wire diameter. The equation of the curve is

$$\tau_0 = 0.52\ d^{1.15} \qquad \text{(unshielded probes)} \tag{4}$$

where d is wire diameter in millimeters and τ_0 is in seconds. The range of scatter of the experimental measurements is shown by the shaded areas. Some of the scatter was attributed to variation in junction bead size. This factor is treated in the discussion section.

Time constant for shielded probes. - The reference time constants τ_0 for the five sizes of shielded probes are also presented in figure 13 as a function of actual wire diameter. A straight line is fit through the data, and the value for each particular probe size taken from the curve fit is presented in table V as a function of nominal wire diameter. The curve fit values for the shielded probes can be expressed by the equation

$$\tau_0 = 1.19\ d^{1.4} \qquad \text{(shielded probes)} \tag{5}$$

where d is wire diameter in millimeters and τ_0 is in seconds.

Radiation Correction

Reference 4 presents a relation to approximate the radiation correction for some simple thermocouple probe configurations, which can be expressed as

$$\text{Radiation correction} \approx \frac{K_{rad}}{\sqrt{Mp/p_0}} \left(\frac{T_i}{T_0}\right)^{3.82} \left[1 - \left(\frac{T_d}{T_i}\right)^4\right] \tag{6}$$

where

K_{rad}	radiation correction coefficient, K
M	stream Mach number
p	stream static pressure, MPa (atm)
p_0	reference static pressure of 0.1 MPa (1 atm)
T_i	probe indicated temperature, K

T_0 reference temperature, 555 K

T_d enclosure duct wall temperature, K

Radiation corrections were experimentally measured for unshielded probes 4 to 10 and for all shielded probes in the apparatus shown in figure 6, and the value of K_{rad} for each probe was calculated by using equation (6). Once the value of K_{rad} has been established, equation (6) can be used to approximate the radiation correction for other conditions of Mach number, pressure, and temperature.

Radiation correction coefficient for unshielded probes. - The values of K_{rad} for unshielded probes 4 to 10 are presented in figure 14 as a function of actual wire diameter. A straight line is fit through the data, and the value for each particular probe size is presented in table VI as a function of nominal wire diameter. The curve fit value of each unshielded probe can be expressed by the relation

$$K_{rad} = 2.5\, d^{0.45} \qquad \text{(unshielded probes)} \tag{7}$$

where d is wire diameter in millimeters.

Radiation correction coefficient for shielded probes. - The values of K_{rad} for the five shielded probes are also presented in figure 14 as a function of actual wire diameter. The values of K_{rad} for all of the shielded probes fall within the scatter-band shown in the figure and can be represented by a single value of 0.8. Size and shield effectiveness are correlated in the discussion section.

Tests on modified shielded probes. - The results of the radiation correction tests (fig. 14 and table VI) for the shielded probes showed that K_{rad} did not decrease with smaller probe sizes as might have been expected. Although the main purpose of this investigation was to examine scaling effects on a given shielded design, two modified probes were built to investigate some hypotheses on design changes to reduce the radiation error. Two probes each of two modified designs were built and tested, both probes were of the wire size (0.32-mm diam) that was used in probe 6.

The first modification was to take a standard shielded probe 6 and increase the bleed area from two 0.79-millimeter-diameter holes to four 0.79-millimeter-diameter holes. This increased the bleed-area-to-inlet-area ratio from 50 percent to 100 percent. It also increased the reference recovery correction factor Δ_0 at Mach 0.9 from 0.003 (standard probe 6) to 0.008. The tests on this probe yielded a K_{rad} of 0.44 as compared with 1.02 obtained for the standard probe 6 (fig. 14).

The second modification was to house a wedge-type thermocouple of the size used in probe 6 (0.32-mm wire diam) in a shield of the size used in probe 9 (i.e., in a 6.35-mm-o.d. shield with a 4.78-mm-diam support). The reference recovery correction factor Δ_0 for this probe remained the same as that for standard shielded probe 9.

The results of the tests on the second modified probe yielded a still lower K_{rad} of 0.37 (fig. 14).

These modifications are treated further in the discussion section.

DISCUSSION

Weld Bead Fabrication

Figure 1 illustrates that after forming the junction, excess material from the weld bead may have to be removed. In fabricating these probes it became increasingly difficult, in the sizes below probe 5 (0.25-mm-diam wire), to control the weld bead size or to dress this bead down without a prohibitive increase in the number of trials to obtain a satisfactory junction. Lack of control of the weld bead size for the smaller probes probably contributed to some of the systematic deviations as well as causing greater scatter in the data.

Recovery Tests

The data for the dependence of Δ_0 on Mach number for both the shielded and unshielded probe designs were in general agreement with the recovery characteristics of similar probe designs of references 3 and 4. However, as mentioned previously for the smaller sizes, the shape and size of the junction weld bead for the unshielded probes would affect the recovery for a given size wire. It was assumed that a smaller bead on a given size wire would result in less stagnation and that the recovery correction would increase. This assumption was checked by carefully dressing down an oversized bead of unshielded probe 3, which had the lowest recovery correction error, and rerunning the recovery test. This resulted in a larger recovery correction, as expected. The magnitude of the increase was 20 percent, which brought the recovery values closer to those of the other sizes.

In addition to pure bending, the exposed wire element and "swept-forward" stem section of the present design (fig. 1) are subject to vibration and sideways deflection when not alined in high-velocity flow. It was suspected that these two factors also contributed to the greater scatter of the recovery data for the smaller probes. Realization of potential wire or probe vibration is important when selecting probes smaller than probe 5 (0.25-mm-diam wire).

The data for pressure effect on recovery (fig. 9) suggest that, for probes as small as probe 1, an individual calibration is required for each probe, rather than reliance on the average data presented.

No experimental determination of the temperature effect on Δ_0 was made. Some earlier work by Simmons (ref. 7) suggested that the value of Δ might be expected to vary with some power n of Reynolds number and hence with $\left(p/T^{1.2}\right)^n$. Simmons' work with long bare wires in crossflow indicated that $n \approx 0.2$. The work of reference 5, however, showed that for the shorter bare wires used in thermocouples, with adjacent supports, the exponent n was smaller than 0.2. In fact, reference 4 gave $n \approx 0.09$ for a crossflow design and $n \approx -0.03$ for a wedge design. In the present work, the average value of n for the median unshielded-wedge curve shown in figure 9 is about 0.1.

Using the relation $\Delta \propto \left(p/T^{1.2}\right)^n$ and having experimentally determined that p^n is $p^{0.1}$, in the absence of experimental data, we made our best estimate of the dependence of Δ on temperature as $\Delta \approx T^{-0.12}$. Thus, at 1400 K, Δ might differ by -16 percent from its value at 300 K. The possible uncertainty in this value is comparable to the possible uncertainty in Δ_0. However, since the value of Δ_0 does not exceed 2.8 percent, the maximum correction for the deviation from the value at 300 K would not exceed 0.45 percent, or 6 K at 1400 K. This is less of an uncertainty than that contributed by uncertainty in the electromotive force of standard-grade type K thermocouple wire.

Time Constant

The data for the unshielded probes (fig. 13) show a curve fit with a slope of 1.15 (τ_0 is a function of wire diameter to the 1.15 power). Examination of the smaller probes showed that the junction beads were not dressed down as indicated in the drawing (fig. 1). Experience has revealed that generally the junction weld beads have a diameter equal to about 3 wire diameters. In order to examine the effect of "dressing down" the bead, the beads of the two probes 3 were dressed down and the time constant tests were rerun. The result was an average 18 percent decrease from the original value of τ_0, for probe 3, plotted in figure 13.

The data plot of the shielded probes (fig. 13) showed a curve fit with a slope of 1.4. The difference in slopes between the shielded and unshielded curve fits is presumed to be due to the effect of the shield. However, the higher time constants for the shielded probes are clearly due to the shielding (which is slower to respond to a gas temperature change) as confirmed by previous results (refs. 4 and 5).

Radiation Tests

The radiation correction coefficient K_{rad} for the unshielded probes showed a systematic decrease with wire diameter (fig. 14). The data showed a curve fit relating K_{rad} to wire diameter to the 0.45 power.

The variation of K_{rad} with wire diameter for the shielded probes, however, was not as expected. Although the shield on a given size probe decreased the radiation loss (as compared with an unshielded probe), K_{rad} did not decrease with wire diameter but remained at approximately 0.8 for all sizes. The average of 0.8 for the shielded probes described here may be compared with the K_{rad} of 1.3 reported in reference 4 for almost the same type of design as treated herein but with a bleed-hole area of 32 percent of the inlet area rather than 50 percent. Although the internal flow of gas in the shield has not been examined in detail, it is suspected that an appreciable amount of "mixing" takes place between the hot gas that is continuously being ingested and some colder boundary layer gas that has "scrubbed" the colder internal walls of the shield. As probe sizes decrease, this mixing may become more pronounced.

Two modified designs of shielded probes were built and tested (see section Tests on modified shielded probes). The first modification, which took a standard shielded probe 6 and increased the bleed area, was modified under the following assumptions:

(1) The internal flow would be increased, thus raising the convective heat transfer rate and consequently the shield temperature.

(2) The faster rate of flow through the shield would decrease the dwell time of the gas and reduce the mixing action. As was previously stated in the text (fig. 14), this modification substantially reduced K_{rad} but at the penalty of raising the recovery correction.

The second modification, which placed a larger shield (equivalent to a probe 9 shield) around a probe 6 size wire, was presumed to reduce K_{rad} below that of probe 6 by reducing the amount of cooled gas that moves from the wall to the wire. The internal cross-sectional flow area of the modified larger shield was increased by a factor of 8 as compared with the standard probe 6 shield. The test results again showed a substantially reduced K_{rad} (fig. 14) over that of standard shielded probe 6, and without the penalty of increasing the recovery correction.

Of the two modifications, the increased bleed hole would be the more realistic for general application since that design would not increase probe size. The second modification could find application where size and flow blockage were not criteria for probe selection.

The results of the two modifications led to the following conclusions:

(1) At an increase in recovery correction, a shielded probe design having a lower K_{rad} could be obtained by increasing the bleed area.

(2) If size were no limit, a design with a large shield (in relation to the size of the thermocouple wire) would provide a lower K_{rad} without an increase in recovery correction.

(3) The general design of a shielded probe as presented in this report is such that all of the internal flow ends at a stagnation region and has to make a right-angle turn to exit through the bleed holes. This would promote mixing of the boundary layer gas with the gas flowing down the center of the tube. In order to decrease this mixing effect, a design that uses an annular bleed area, where the boundary layer gas can exit without turning, may improve radiation shielding efficiency (fig. 15). It may also lessen the influence of the recovery of the shield on wire recovery through a decrease in gas conduction from shield to wire.

CONCLUDING REMARKS

A review of the characteristics of the two probe designs presented in this report clearly shows that the selection of a probe for a given application involves compromises among several characteristics. For a given size, the unshielded-wedge design has a faster time constant and the recovery characteristics are less affected by flow misalinement and by operation over a large pressure range. The shielded probes afford better physical protection to the thermocouple element and have, especially for the larger sizes, substantially decreased recovery and radiation corrections.

Attempting to use smaller probes yielded some unexpected results. Difficulty was encountered in controlling the size and shape of the welded junction bead; this resulted in a 20 percent increase in measured time constant for a given size wire. In regard to radiation correction, the smaller shielded probes did not show a decrease in radiation correction as might have been expected. Two modified shielded probes that showed improved radiation characteristics were introduced into the investigation, and a third design (not tested) was proposed.

Also, for the smaller probes special consideration must be made in high-density or high-velocity subsonic flows in regard to structural characteristics. Under high loading, stem immersion lengths must be kept short to prevent the stream from bending the stem back. Also, the exposed wire element (for the unshielded design) and the swept-forward stem section of both designs are subject to vibration and sideways deflection when not accurately alined in a high-velocity flow.

The two general probe designs presented in this report, as well as the modified designs, can be applied as individual elements or "stacked" to form multielement rakes. The range of sizes and characteristics of the probes presented gives a wide selection for many applications in various flow fields.

Lewis Research Center,
National Aeronautics and Space Administration,
Cleveland, Ohio, September 30, 1977,
505-04.

REFERENCES

1. Moffat, Robert J.: Gas Temperature Measurement. Temperature - Its Measurement and Control in Science and Industry, Charles M. Herzfeld, ed., Reinhold Publishing Corp., Vol. 3, Part 2, 1962, pp. 553-571.

2. Scadron, Marvin D.; and Warshawsky, Isidore: Experimental Determination of Time Constants and Nusselt Numbers for Bare-Wire Thermocouples in High-Velocity Air Streams and Analytic Approximation of Conduction and Radiation Errors. NACA TN 2599, 1952.

3. Stickney, Truman M.: Recovery and Time-Response Characteristics of Six Thermocouple Probes in Subsonic and Supersonic Flow. NACA TN 3455, 1955.

4. Glawe, George E.; Simmons, Frederick S.; and Stickney, Truman M.: Radiation and Recovery Corrections and Time Constants of Several Chromel-Alumel Thermocouple Probes in High-Temperature, High-Velocity Gas Streams. NACA TN 3766, 1956.

5. Scadron, Marvin D.; Warshawsky, Isidore; and Gettelman, Clarence C.: Thermocouples for Jet-Engine Gas Temperature Measurement. Proc. Instrum. Soc. Am., vol. 7, Paper 52-12-3, 1952, pp. 142-148.

6. Glawe, George E.; Johnson, Robert C.; and Krause, Lloyd N.: Intercomparison of Several Pyrometers in a High-Temperature Gas Stream. Temperature, Its Measurement and Control in Science and Industry, Charles M. Herzfeld, ed., Reinhold Publishing Corp., Vol. 3, Part 2, 1962, pp. 601-605.

7. Simmons, Frederick S.: Recovery Corrections for Butt-Welded, Straight-Wire Thermocouples in High-Velocity, High-Temperature Gas Streams. NACA RM E54G22a, 1954.

TABLE I. - NOMINAL PROBE DIMENSIONS

Probe	Swaged assembly outside diameter, mm	Nominal wire size		Shield size		Z	Y	X	W	V	U	Twice sheath outside diameter, minimum, T_R, mm	Drill size, S		Number of bleed holes, R
		Brown & Sharp gage	Diameter, mm	Outside diameter, mm	Wall thickness, mm	Dimension (table II), mm							Drill number	Diameter, mm	
1	0.25	48	0.032	----	----	0.51	(a)	----	----	-----	(a)	0.51	--	----	--
2	.30	38	.101	----	----	1.53		----	----	-----		1.02	--	----	--
3	.81	36	.13	----	----	1.91		----	----	-----		1.57	--	----	--
4	1.02	34	.16	1.63	0.30	2.41		0.51	2.03	5.59		2.03	76	0.51	2
5	1.27	30	.25	----	----	3.81		----	----	-----		2.54	--	----	--
6	1.57	28	.32	2.28	.32	4.83		.79	3.18	9.53		3.18	68	.79	2
7	2.29	26	.41	3.18	.46	6.10		.79	3.96	12.4		4.57	68	.79	4
8	3.18	24	.51	3.96	.51	7.62		1.07	5.03	15.5		6.35	58	1.07	4
9	4.78	20	.81	6.35	.89	12.2		1.57	7.92	24.9		9.53	52	1.57	4
10	6.35	18	1.02	----	----	15.2		----	----	-----		12.7	--	----	--

[a]As required.

TABLE II. - DESIGN CONSTRAINTS

Dimension	Relation
Z	15 Times wire diameter
S	Bleed-hole diameter
X	Linear dimension equal to S
W	Shield outside diameter plus X
V	Z plus twice shield outside diameter
T_R	2 Times sheath outside diameter, minimum
Y	1 Shield outside diameter, minimum, for shielded probe
U	Probe support length, as required

TABLE III. - REFERENCE RECOVERY CORRECTION FACTORS AT SELECTED MACH NUMBERS FOR UNSHIELDED THERMOCOUPLE PROBES

[Experimental values.]

Probe	Mach number		
	0.3	0.6	0.9
	Reference recovery correction factor, Δ_0		
1	0.003	0.0125	0.021
2	.003	.011	.021
3	.0025	.0095	.017
4	.003	.0125	.025
5		.0125	.024
6		.0115	.022
7		.011	.021
8		.011	.024
9		.012	.028
10		.0125	.027

TABLE IV. - REFERENCE RECOVERY CORRECTION FACTORS AT SELECTED MACH NUMBERS FOR SHIELDED THERMOCOUPLE PROBES

[Experimental values.]

Probe	Mach number		
	0.3	0.6	0.9
	Reference recovery correction factor, Δ_0		
4	0.004	0.003	0.005
6	↓	.002	.003
7		.002	.003
8		.002	.003
9	.0005	.001	.002

TABLE V. - REFERENCE TIME CONSTANTS FOR UNSHIELDED AND SHIELDED THERMOCOUPLE PROBES

[Smoothed values.]

Probe	Nominal wire diameter, mm	Unshielded probes	Shielded probes
		Reference time constant, τ_0, sec	
1	0.03	0.010	-----
2	.10	.037	-----
3	.13	.050	-----
4	.16	.063	0.092
5	.25	.106	-----
6	.32	.140	.241
7	.41	.187	.342
8	.51	.240	.464
9	.81	.408	.886
10	1.02	.532	-----

TABLE VI. - RADIATION CORRECTION COEFFICIENTS FOR UNSHIELDED AND SHIELDED THERMOCOUPLE PROBES

[Smoothed values.]

Probe	Nominal wire diameter, mm	Unshielded probes	Shielded probes
		Radiation correction coefficient, K_{rad}, K	
4	0.16	1.10	0.80
5	.25	1.34	----
6	.32	1.50	.80
7	.41	1.67	↓
8	.51	1.85	
9	.81	2.27	
10	1.02	2.52	----

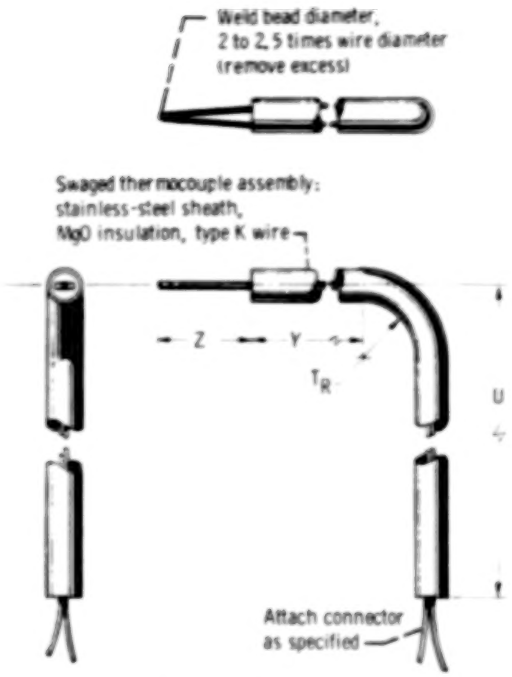

(a) Unshielded wedge.

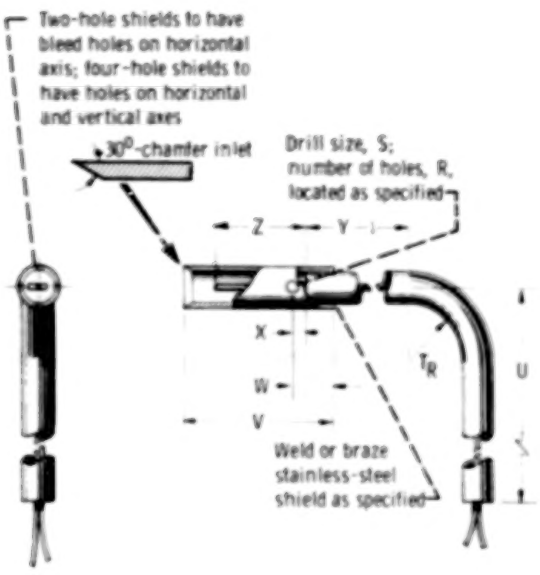

(b) Shielded wedge.

Figure 1. - Design details of shielded and unshielded thermocouple probes. (Probes subjected to high humidity should be baked at 425 K for 4 hr and a sealant applied to insulation at each end of swaged assembly.)

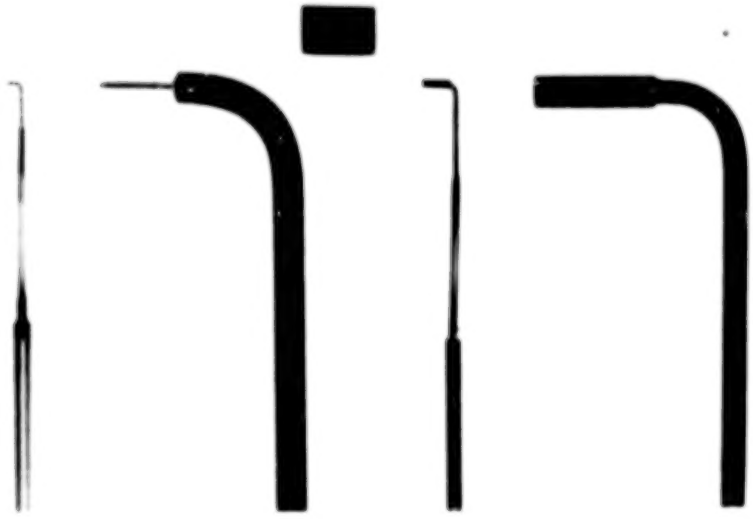

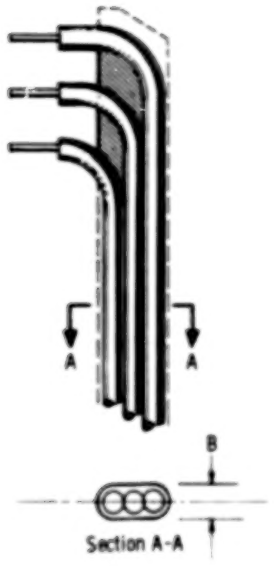

Figure 3. - Multisensing probe assembly.

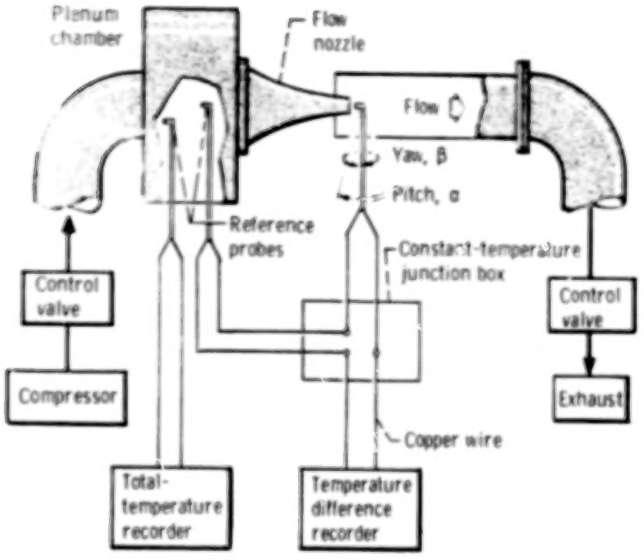

Figure 4. - Recovery test apparatus.

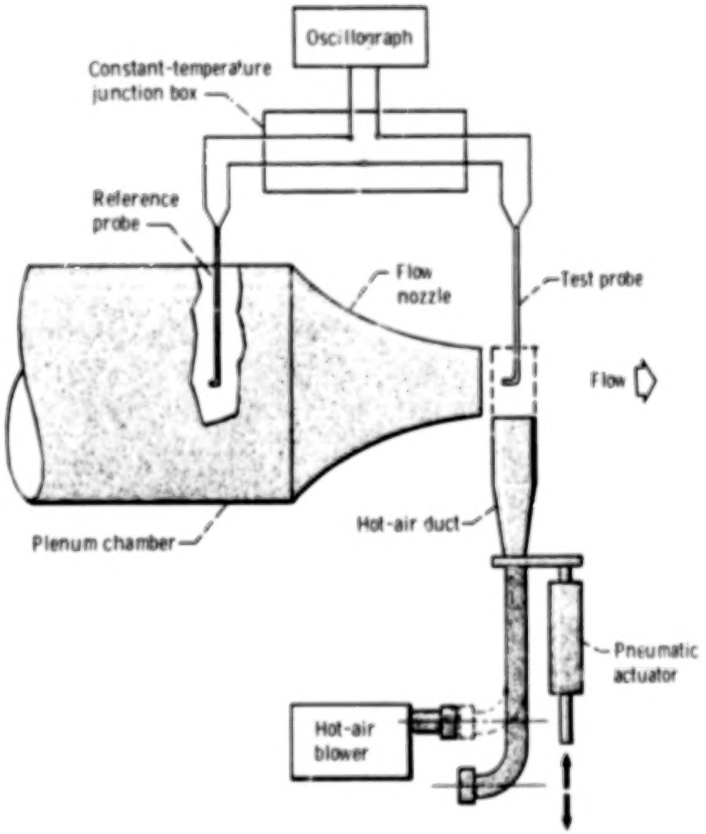

Figure 5. - Time-constant test apparatus.

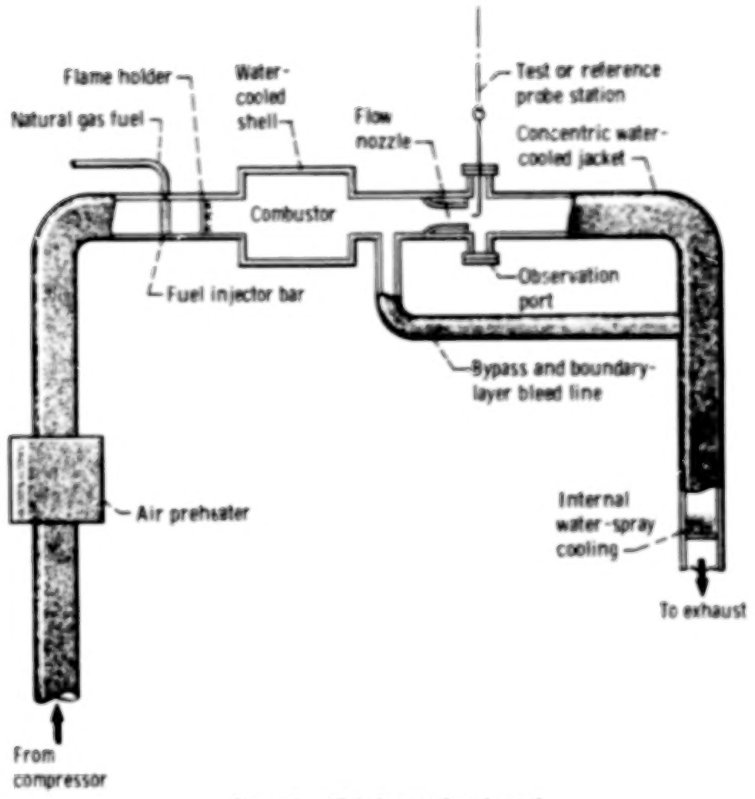

Figure 6. - High-temperature tunnel.

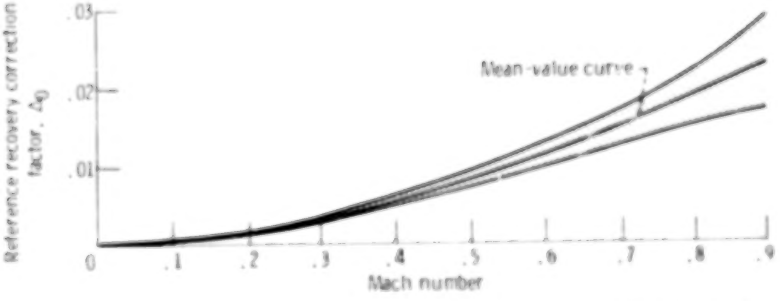

Figure 7. - Reference recovery correction factor as function of Mach number for unshielded wedge-type thermocouple probes.

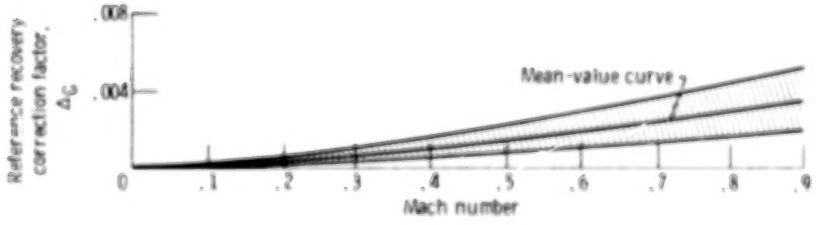

Figure 8. - Reference recovery correction factor as function of Mach number for shielded wedge-type thermocouple probes.

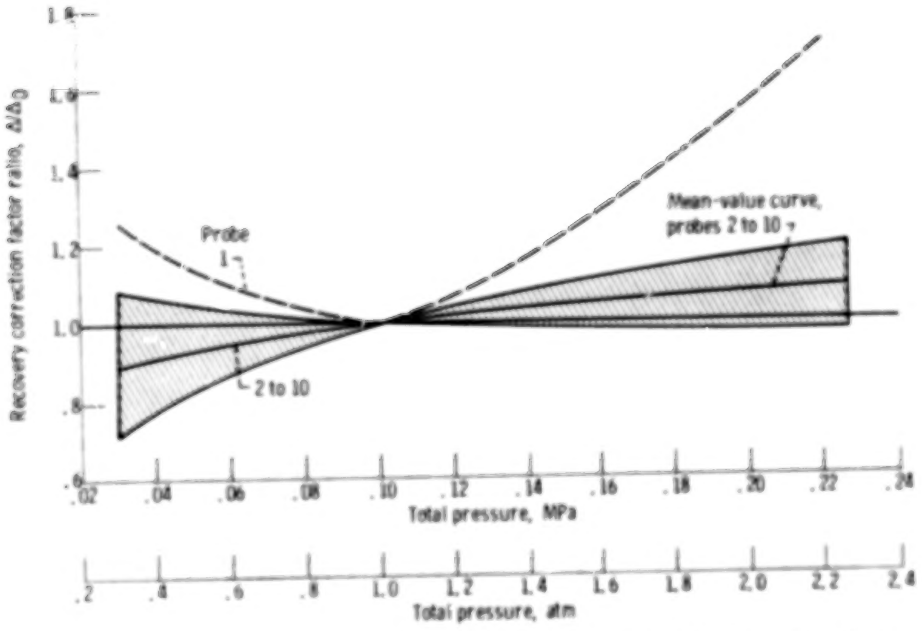

Figure 9. - Variation of recovery correction factor with pressure for unshielded wedge-type thermocouple probes.

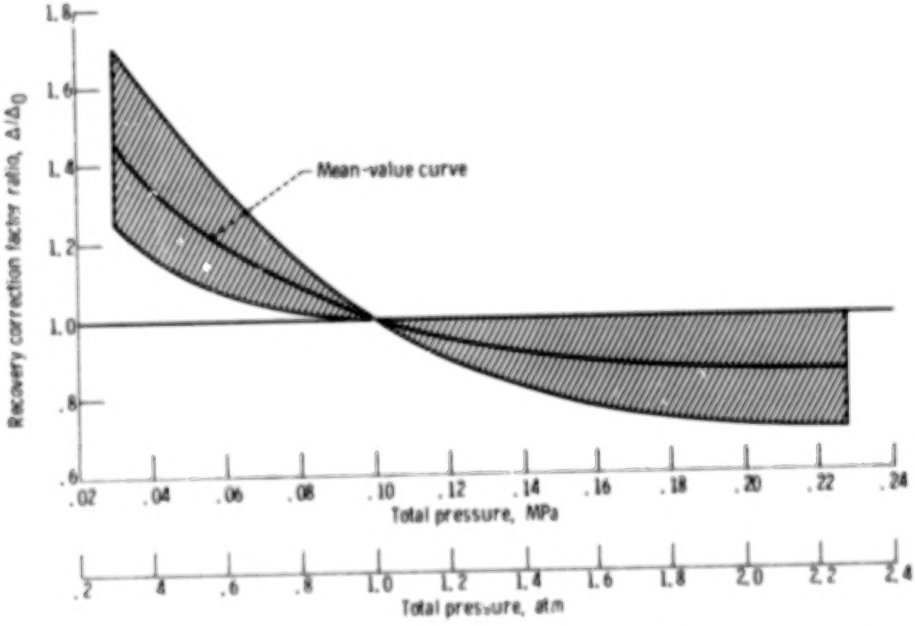

Figure 10. - Variation of recovery correction factor with pressure for shielded wedge-type thermocouple probes.

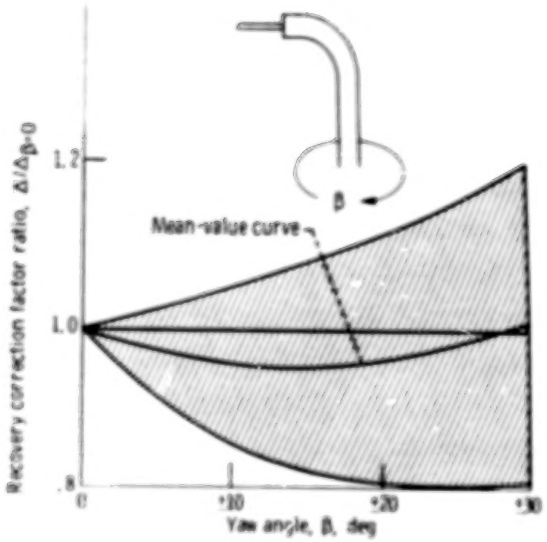

Figure 11. - Variation of recovery correction factor with yaw angle for unshielded wedge-type thermocouple probes.

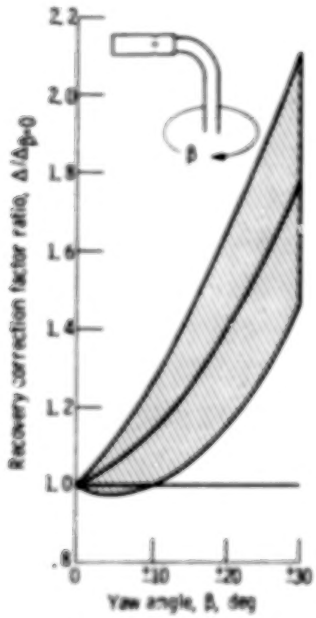

Figure 12. - Variation of recovery correction factor with yaw angle for shielded wedge-type thermocouple probes.

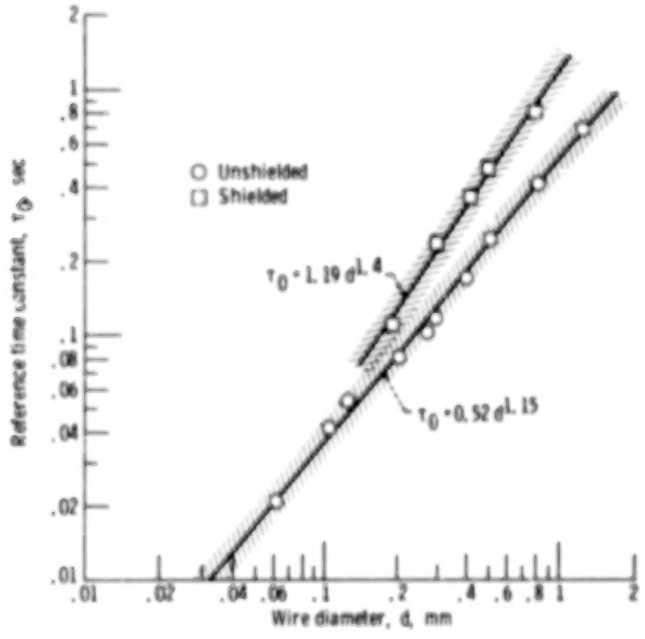

Figure 13. - Reference time constant as function of wire diameter for unshielded and shielded thermocouple probes.

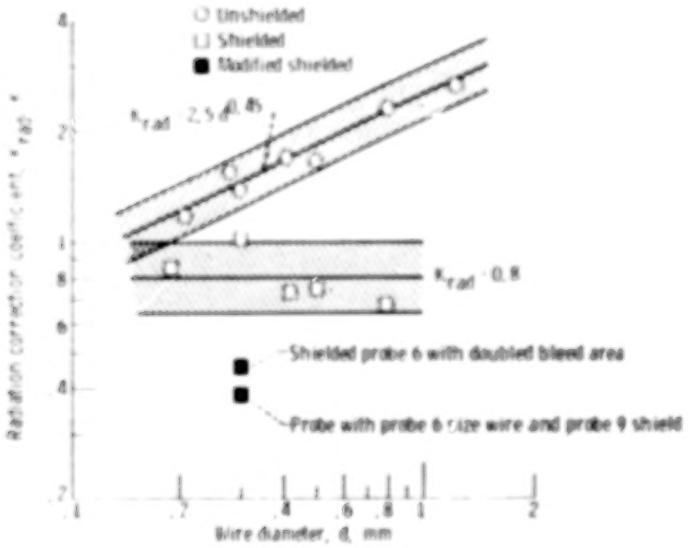

Figure 14. Radiation correction coefficient as function of wire diameter for shielded and unshielded probes.

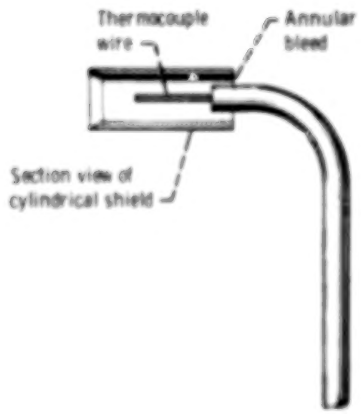

Figure 15. - Head detail of proposed shielded-probe design with annular bleed.

1. Report No.	2. Government Accession No.	3. Recipient's Catalog No.
NASA TP-1099		

4. Title and Subtitle	5. Report Date
RECOVERY AND RADIATION CORRECTIONS AND TIME CONSTANTS OF SEVERAL SIZES OF SHIELDED AND UNSHIELDED THERMOCOUPLE PROBES FOR MEASURING GAS TEMPERATURE	January 1978
	6. Performing Organization Code

7. Author(s)	8. Performing Organization Report No.
George E. Glawe, Raymond Holanda, and Lloyd N. Krause	E-9289
	10. Work Unit No. 505-04

9. Performing Organization Name and Address	11. Contract or Grant No.
National Aeronautics and Space Administration Lewis Research Center Cleveland, Ohio 44135	
	13. Type of Report and Period Covered: Technical Paper

12. Sponsoring Agency Name and Address	14. Sponsoring Agency Code
National Aeronautics and Space Administration Washington, D.C. 20546	

15. Supplementary Notes

16. Abstract

Performance characteristics were experimentally determined for several sizes of a shielded and unshielded thermocouple probe design. The probes are of swaged construction and were made of type K wire with a stainless-steel sheath and shield and MgO insulation. The wire sizes ranged from 0.03- to 1.02-mm diameter for the unshielded design and from 0.16- to 0.81-mm diameter for the shielded design. The probes were tested through a Mach number range of 0.2 to 0.9, through a temperature range of room ambient to 1420 K, and through a total-pressure range of 0.03 to 0.22 MPa (0.3 to 2.2 atm). Tables and graphs are presented to aid in selecting a particular type and size. Recovery corrections, radiation corrections, and time constants were determined.

17. Key Words (Suggested by Author(s))	18. Distribution Statement
Temperature measuring instruments Gas temperature measurement Thermocouple probe	Unclassified - unlimited STAR Category 35

19. Security Classif. (of this report)	20. Security Classif. (of this page)	21. No. of Pages	22. Price*
Unclassified	Unclassified	25	A02

* For sale by the National Technical Information Service, Springfield, Virginia 22161

NASA-Langley, 1978